Zebrafish as a Model for Studying Age-Dependent Sarcopenia and Frailty

Paula Aranda-Martínez , Ramy K. A. Sayed , José Fernández-Martínez , Yolanda Ramírez-Casas , Yang Yang , Germaine Escames , Darío Acuña-Castroviejo *

Posted Date: 16 May 2024

doi: 10.20944/preprints202405.1073.v1

Keywords: zebrafish; aging; skeletal muscle; mitochondria; sarcopenia

Article

Zebrafish as a Model for Studying Age-Dependent Sarcopenia and Frailty

Paula Aranda-Martínez [1,2,3], Ramy K. A. Sayed [4], José Fernández-Martínez [1,2,3], Yolanda Ramírez-Casas [1,2,3], Yang Yang [5], Germaine Escames [1,2,3,6] and Darío Acuña-Castroviejo [1,2,3,6,7,*]

1 Centro de Investigación Biomédica, Facultad de Medicina, Departamento de Fisiología, Universidad de Granada, 18016 Granada, Spain; ampaula@correo.ugr.es (P.A.-M.); josefermar@ugr.es (J.F-M.); yolandaramirez@ugr.es (Y.R.-C.); gescames@ugr.es (G.E.)
2 Instituto de Biotecnología, Parque Tecnológico de Ciencias de la Salud, Universidad de Granada, 18016 Granada, Spain
3 Instituto de Investigación Biosanitaria (Ibs. Granada), Hospital Universitario San Cecilio, 18016 Granada, Spain
4 Department of Anatomy and Embryology, Faculty of Veterinary Medicine, Sohag University, Sohag 82524, Egypt; ramy.kamal@vet.sohag.edu.eg
5 Key Laboratory of Resource Biology and Biotechnology in Western China, Ministry of Education, Faculty of Life Sciences and Medicine, Northwest University, 710069 Xi'an, China; yang200214yy@163.com
6 Centro de Investigación Biomédica en Red de Fragilidad y Envejecimiento Saludable (CIBERFES), Instituto de Salud Carlos III (ISCIII), 28029 Madrid, Spain
7 UGC de Laboratorios Clínicos, Hospital Universitario San Cecilio, 18016 Granada, Spain
* Correspondence: dacuna@ugr.es

Abstract: Currently, there is an increase in the aging of the population, which represents a risk factor for many diseases, including sarcopenia. Sarcopenia involves progressive loss of mass, strength, and function of the skeletal muscle. Some mechanisms include alterations in muscle structure, reduced regenerative capacity, oxidative stress, mitochondrial dysfunction, and inflammation. The zebrafish has emerged as a new model for studying skeletal muscle aging because of its numerous advantages, including histological and molecular similarity to human skeletal muscle. In this study, we used fish of 2, 10, 30, and 60 months of age. The older fish showed a higher frailty index because of reduced locomotor activity and alterations in biometric measurements. We observed changes in muscle structure with a decreased number of myocytes and an increase in collagen with aging, corresponding to alterations in the synthesis, degradation, and differentiation pathways. These changes were accompanied by mitochondrial alterations, such as a decrease in intermyofibrillar mitochondria, increased mitochondrial damage, and reduced mitochondrial dynamics. Overall, we demonstrated a similarity in the aging processes of muscle aging between zebrafish and mammals.

Keywords: zebrafish; aging; skeletal muscle; mitochondria; sarcopenia

1. Introduction

The life expectancy of the population is significantly increasing, and by 2030, one out of six people worldwide will be 60 years old or older, whereas the population aged 60 years or over will double by 2050, and the population aged 80 years or over will triple. Aging is a major risk factor for numerous diseases, including sarcopenia, which is characterized by the progressive loss of skeletal muscle mass, strength, and function, leading to functional impairment, frailty, and increased mortality [1]. Thus, it is reasonably expected that there will be an increase in sarcopenia and sarcopenia-related deaths in the next years. Although the exact mechanisms of sarcopenia are not fully understood, it is known to involve alterations in muscle structure and function, reduced regenerative capacity, oxidative stress and inflammation, and mitochondrial [2].

Although we are not aware of any studies that provide an established treatment or definitive diagnosis for this condition, preventive approaches, including exercise and increased protein intake, have been recommended [3]. Therefore, the use of improved and diverse animal models is imperative for gaining a comprehensive understanding of its pathogenesis. While rodents are the most used

 doi:10.20944/preprints202405.1073.v1

models for studying sarcopenia, alternative models such as Drosophila and C. elegans have been proposed because of their cost-effectiveness and shorter lifespans. However, it should be noted that these alternative models differ more from human skeletal muscle. Here, the zebrafish emerges as a novel and promising model to consider [4].

We have previously demonstrated in an aged mouse model that there is a reduction in type II muscle fibers, muscle fiber hypertrophy, and collagen infiltrations, which contribute to the loss of muscle mass and function [5]. Additionally, we observed a decreased mitochondrial number, in addition to mitochondrial damage such as disrupted cristae and swelling. There was also a reduction in lactate content and an increase in apoptotic nuclei [6]. Subsequently, we identified the pivotal role of the NLRP3 inflammasome in the development of sarcopenia [7]. More recently, we investigated the connection between sarcopenia and chronodisruption, specifically focusing on the loss of Bmal1 [8], as it plays a crucial role in the maintenance and repair of skeletal muscle [9,10]

Zebrafish have emerged as a promising new model for studying sarcopenia because of their numerous advantages [11] and extensive application in aging research [12]. Notably, zebrafish skeletal muscle exhibits striking similarities to human muscle in both histological and molecular aspects [13]. Additionally, exercise can reduce age-related sarcopenia in zebrafish [14,15]. Consequently, we advocate the use of zebrafish as a novel model to investigate the physiology of aging, particularly in relation to skeletal muscle, with the aim of establishing an effective diagnostic protocol and treatment for sarcopenia.

2. Results

2.1. Morphometric and Motor Activity Analysis Revealed a Decline in Physical Condition and a Concurrent Increase in Frailty with Aging

As expected, there was a progressive increase in BMI with age, which can be attributed to the increase in weight and length (Figure 1). Interestingly, the groups aged 2 and 10 months did not display significant differences in BMI, despite the 10-month-old group having greater weight and length, although a trend to increase was observed in the latter (Figure 1). Notably, the BMI was significantly higher in the 30-month-old fish than in the 2-month-old fish, although it did not differ significantly from the 10-month-old group (Figure 1A). However, the total weight and total length of the 30-month-old group did present differences among both groups (Figure 1B,C). Finally, the 60-month group showed a significant increase in BMI, which corresponded to a likewise significant increase in weight and length (Figure 1).

The locomotor activity recorded by the video-tracking open-field test did not reveal changes in the 2- and 10-month groups in terms of total distance (Figure 1D), maximum speed (Figure 1E), or mean speed (Figure 1F). The total distance was significantly reduced in the 30- and 60-month groups compared with the 10-month group (Figure 1D). Furthermore, significant changes were observed in the maximum speed of the 60-month group compared with the 2- and 10-month groups (Figure 1E). Lastly, age also influenced mean speed, which exhibited a significant reduction in the 30- and 60-month groups, contrasting with the 2- and 10-month groups (Figure 1F).

The frailty index is commonly employed in the clinic to assess the level of vulnerability of patients. Recently, this measure has been translated to primates and mice [6,16], and we have now adapted it to zebrafish. The aforementioned morphometric and locomotor measurements were used to calculate the frailty index (FI). Age exhibited an impact on the frailty index, with an increase observed at 30 months of age compared with the 2- and 10-month groups, and this increase was statistically significant at 60 months (Figure 1G). You can find all the data in Supplementary Table S1.

 doi:10.20944/preprints202405.1073.v1

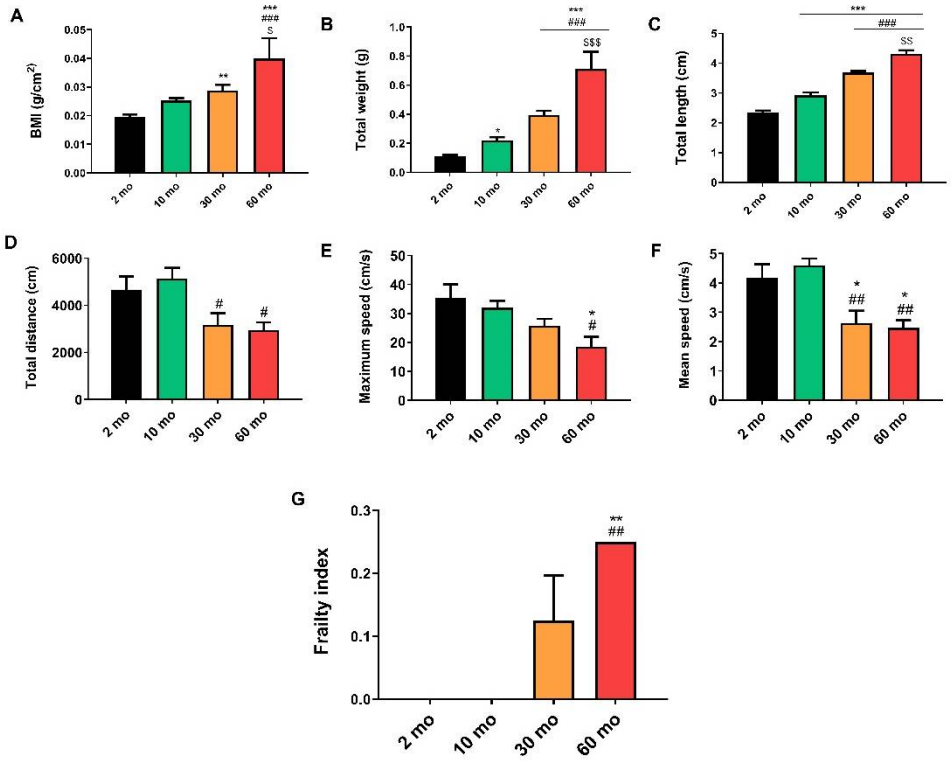

Figure 1. Increase in frailty index with age. (**A**) BMI (g/cm²) increased significantly in 30 and 60-month groups. (**B**) Total weight (g) and (**C**) total length (cm) increased in an age-dependent manner. (**D**) Total distance (cm) decreased significantly in 30 and 60-month groups regarding younger groups. (**E**) Maximum speed (cm/s) underwent a tendency to decrease, being significant in the oldest group with respect to 2 and 10 month-groups. (**F**) Mean speed (cm/s) showed a prominent decrease in the 30-month group and remained in the 60-month group relative to young groups. (**G**) The groups of 2 and 10 months had a frailty index to 0. However, at 30 months we observed an increase, which became significant at 60 months. Data are presented as mean ± SEM. * $p < 0.05$ vs. 2 mo; ** $p < 0.01$ vs. 2 mo; *** $p < 0.001$ vs. 2 mo; # $p < 0.05$ vs. 10 mo; ## $p < 0.01$ vs. 10 mo; ### $p < 0.001$ vs. 10 mo; $ $p < 0.05$ vs. 30 mo; $$ $p < 0.01$ vs. 30 mo; $$$ $p < 0.001$ vs. 30 mo. One-way ANOVA with a Tukey's post hoc test.

2.2. The Structure and Organization of the Zebrafish Skeletal Muscle Are Significantly Compromised with Age

Light microscopy images of longitudinal sections stained with hematoxylin and eosin (H&E) stain showed a normal structure and organization of zebrafish skeletal muscle fibers in the 2- and 10-month groups (Figure 2A), with no differences in the number of myocytes (Figure 2B) but an increase in myocyte width at 10 months (Figure 2C). At 30 months, while there was still good organization of the fibers (Figure 2A), hypertrophy of myocytes was observed, which was related to a reduction in the number of myocytes (Figure 2B) and an increase in the myocyte width (Figure 2C). In contrast, older fish exhibited disorganization of the skeletal muscle and an increase in connective tissue (Figure 2A), resulting in a significant decrease in the number of myocytes compared with the other groups (Figure 2B) and a narrower width compared with the 10- and 30-month groups (Figure 2C).

On the other hand, VG staining revealed low collagen content in the 2 and 10 groups (Figure 2D and 2E). In contrast, an age-related increase in collagen content was detected, with a slight increase at 30 months and a more substantial increase at 60 months (Figure 2D and 2E).

 doi:10.20944/preprints202405.1073.v1

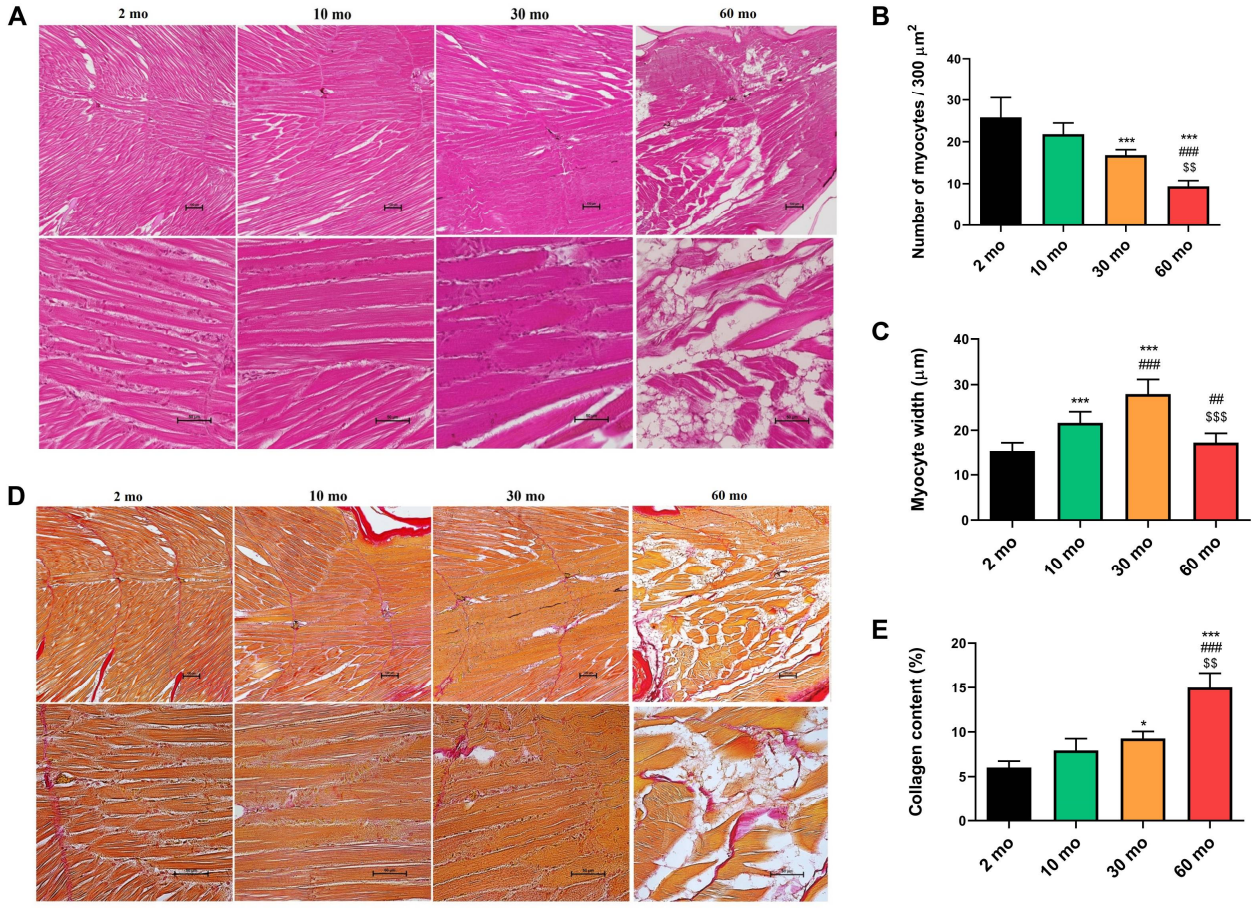

Figure 2. Histological and morphometric changes of zebrafish skeletal muscle. (**A**) Light microscopy images of longitudinal sections stained with hematoxylin and eosin (H&E) displayed a normal structure in the 2 and 10-month groups, whereas in the 30-month group, we observed hypertrophy, and at 60 months, muscle disorganization and atrophy. (**B**) The number of myocytes decreased with age. (**C**) The width of the myocytes increased at 10 and 30 months. (**D**) Light microscopy images of longitudinal sections stained with Van Gieson (VG) highlighted collagen infiltrations in red. (**E**) Collagen content exhibited a significant increase in 60-month-old fish. Data are presented as mean ± SEM. * $p < 0.05$ vs. 2 mo; *** $p < 0.001$ vs. 2 mo; ### $p < 0.001$ vs. 10 mo; $$ $p < 0.01$ vs. 30 mo; $$$ $p < 0.001$ vs. 30 mo. One-way ANOVA with a Tukey's post hoc test.

2.3. Pathways of Muscle Growth and Differentiation Undergo Alterations with Aging in Zebrafish

Muscle protein synthesis is modulated by the Akt/mTOR/p70s6k pathway, which is affected by age in mammals [17,18]. We analyzed the gene expression of akt and p70s6k to study how aging impacted this pathway in zebrafish skeletal muscle. Concerning akt, we observed an age-dependent reduction in its expression, which was significant in the 30 and 60 months groups compared with the younger group (Figure 3A). Because p70s6k acts downstream of akt and is one of the final steps of the pathway [19], it exhibited a marked decrease in the 10, 30, and 60-month groups compared with the 2-month group (Figure 3B).

In addition, we investigated whether aging had an impact on muscle growth and differentiation pathways in zebrafish. Myogenin, which plays a key role in muscle myogenesis [20], exhibited a progressive reduction with statistical significance at 60 months compared with the 2- and 10-month groups (Figure 3C). On the other hand, prdm1a is a repressor of fast muscle fiber differentiation and a promoter of slow fiber differentiation [21,22]. We observed a tendency to increase its expression in the two oldest groups, although the difference was not significant (Figure 3D).

 doi:10.20944/preprints202405.1073.v1

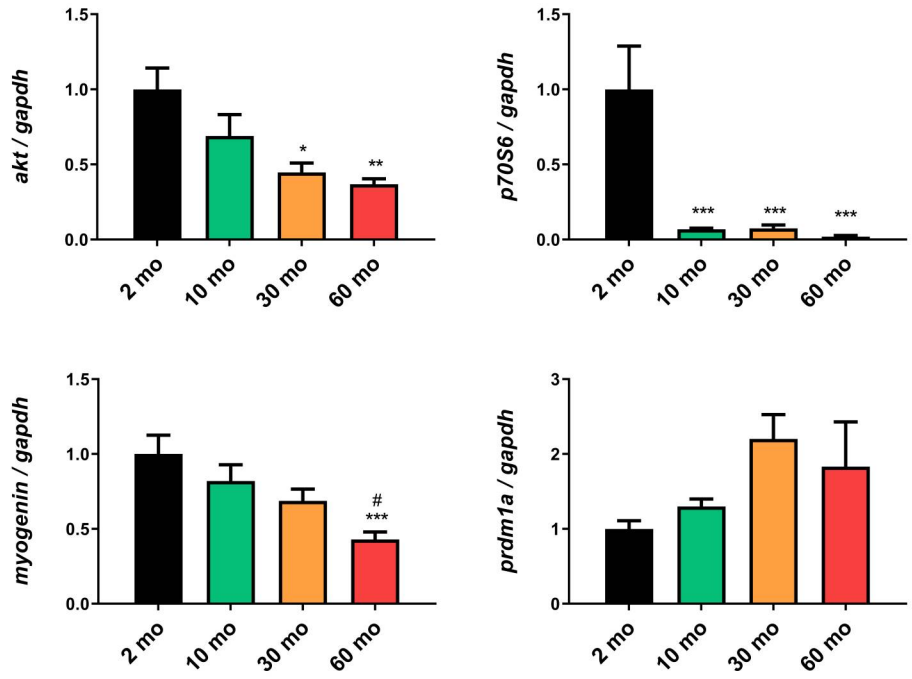

Figure 3. Disruption of muscle growth and differentiation pathways during aging. (**A**) akt expression showed an age-dependent decrease. (**B**) p70s6k was significantly reduced as early as 10 months of age. (**C**) myogenin expression demonstrated a progressive reduction, with statistical significance observed at 60 months. (**D**) prdm1a increased at 30 and 60 months but not statistically significant. Data are presented as mean ± SEM. * $p < 0.05$ vs. 2 mo; ** $p < 0.01$ vs. 2 mo; # $p < 0.05$ vs. 10 mo. One-way ANOVA with a Tukey's post hoc test.

2.4. Zebrafish Aging Revealed Alterations in the Ultrastructure of Muscle and Mitochondria

Electron microscopy examination of 2-month-old fish revealed the normal ultrastructure of the skeletal muscle (Figure 4A), which comprises longitudinally arranged myofibrils (Mf). However, some myofibrils were detected to be ill-developed, with disorganized my filaments and intermyofibrillar components (black asterisk). The intermyofibrillar spaces displayed a sarcoplasmic reticulum (SR), transverse tubules (T) forming a terminal cisterna (C), and intermyofibrillar mitochondria (IFM). Both IFM and subsarcolemmal mitochondria (SSM) were compacted and showed well-organized cristae. The nucleus (N) was observed in its usual peripheral position beneath the sarcolemma (black arrow).

At the age of 10 months, the muscle was fully developed and characterized by well-aligned myofibrils and sarcomeres (Figure 4A). Transverse tubules were normally formed, the SR network was well organized, and the nucleus was positioned normally. The IFMs were compacted and exhibited organized cristae. However, individual cases revealed vacuolation (white arrow). Numerous small-sized membranous vacuoles (v) of possibly autophagic nature were observed among the SSM, which remained entirely normal and compacted. Less interstitial connective tissue (In) and glycogen droplets (g) are also depicted.

The skeletal muscles of 30-month-old fish demonstrated organized myofibril and sarcomere alignment (Figure 4A). Hypertrophy was observed in both the IFM and SSM, with normally arranged cristae. However, few ones exhibited indistinct cristae (white asterisk). Numerous vacuoles and swelling of the SR and triads were evident. Moreover, shrinkage of the peripherally positioned nucleus was observed.

At the age of 60 months, myofibril disorganization and adjacent sarcomere misalignment were demonstrated, with the presence of wide intermyofibrillar spaces and swelling of SR. Both IFM and SSM displayed abnormal structures and were entirely vacuolated with damaged and/or disorganized cristae (Figure 4A).

Morphometric analysis revealed a significant reduction in the length of sarcomeres compared with those of 2-month-old fish (Figure 4B). The number and cross-sectional area (CSA) of IFM were significantly decreased at the age of 60 months (Figure 4C,D). However, the number of SSM was

 doi:10.20944/preprints202405.1073.v1

significantly increased at the age of 30 months, whereas CSA showed non-significant differences (Figure 4E,F). Bands A and H increased significantly in 60-month-old fish (Figure 4G,H), whereas band I decreased (Figure 4I). Finally, a pronounced increase in the percentage of damaged mitochondria in aged muscle was observed, reaching 100% at 60 months (Figure 4J).

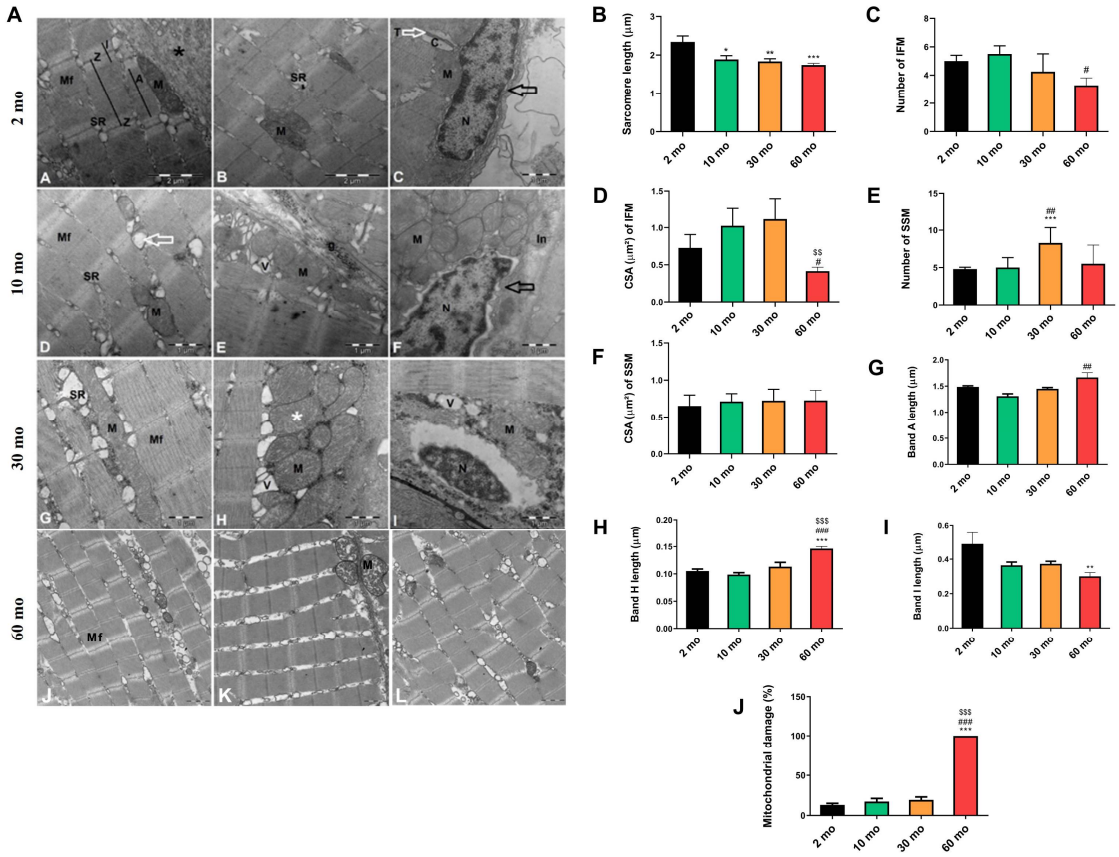

Figure 4. Changes in muscle ultrastructure and mitochondria. (**A**) Electron micrograph of a longitudinal ection of the skeletal muscle of 2-month-old fish depicted myofibrils (Mf), isotropic bands (I), anisotropic bands (A) sarcomere between each two successive Z-Line (Z), sarcoplasmic reticulum (SR) and mitochondria (M). An area of ill-developed myofibrils was detected (black asterisk) and the triad region, formed by transverse tubules (T and white arrow) and terminal cisterns (C), was evident. The nucleus (N) was peripherally located under the sarcolemma (black arrow). At age of 10 months-old we observed normal myofibrils (Mf), sarcoplasmic reticulum (SR) and mitochondria (M), with presence of vacuolated mitochondria (white arrow), vacuoles (V), glycogen droplets (g), peripherally positioned nucleus (N) under the sarcolemma (black arrow) and interstitial tissues (In). 30 months-old fishes presented normal myofibrils (Mf), swollen sarcoplasmic reticulum (SR) and hypertrophied mitochondria (M), with presence of indistinct mitochondrial cristae (white asterisk), vacuoles (V), and shrinkage of nucleus (N). 60 months-old group showed disorganized myofibrils (Mf), mitochondria (M), with presence of damage ones and others with damaged and/or disorganized cristae as well as vacuoles (V). (**B**) Sarcomere length decreased with age. (**C**) The number of IFM and (**D**) their CSA decreased significantly at 60 months of age. (**E**) The number of SSM increased at 30-month group. (**F**) No difference was found in the CSA of SSM. (**G**) Band A length increased in 60-month-old fish, (**H**) as did the H band. (**I**) The length of the I band decreased in the 60-month group. (**J**) Mitochondrial damage increased sharply in the older group. Data are presented as mean ± SEM. * $p < 0.05$ vs. 2 mo; ** $p < 0.01$ vs. 2 mo; *** $p < 0.001$ vs. 2 mo; # $p < 0.05$ vs. 10 mo; ## $p < 0.01$ vs. 10 mo; ### $p < 0.001$ vs. 10 mo; $$ $p < 0.01$ vs. 30 mo; $$$ $p < 0.001$ vs. 30 mo. One-way ANOVA with a Tukey's post hoc test.

Through TEM analysis, we observed a decline in the number of mitochondria in the muscle with aging. Our investigation also delved into whether crucial processes for preserving mitochondrial

 doi:10.20944/preprints202405.1073.v1

homeostasis, such as mitochondrial dynamics, were affected. In terms of mitochondrial fusion, we observed a trend of decreasing expression of mfn1 (Figure 5A) and opa1 (Figure 5B) with age, which became significantly reduced at 60 months. Conversely, when examining mitochondrial fission, we found an increase in the expression of dyn2 (Figure 5C) and drp1 (Figure 5D) at 10 and 30 months, respectively, but their expression sharply decreased at 60 months, mirroring the pattern observed with mitochondrial fusion.

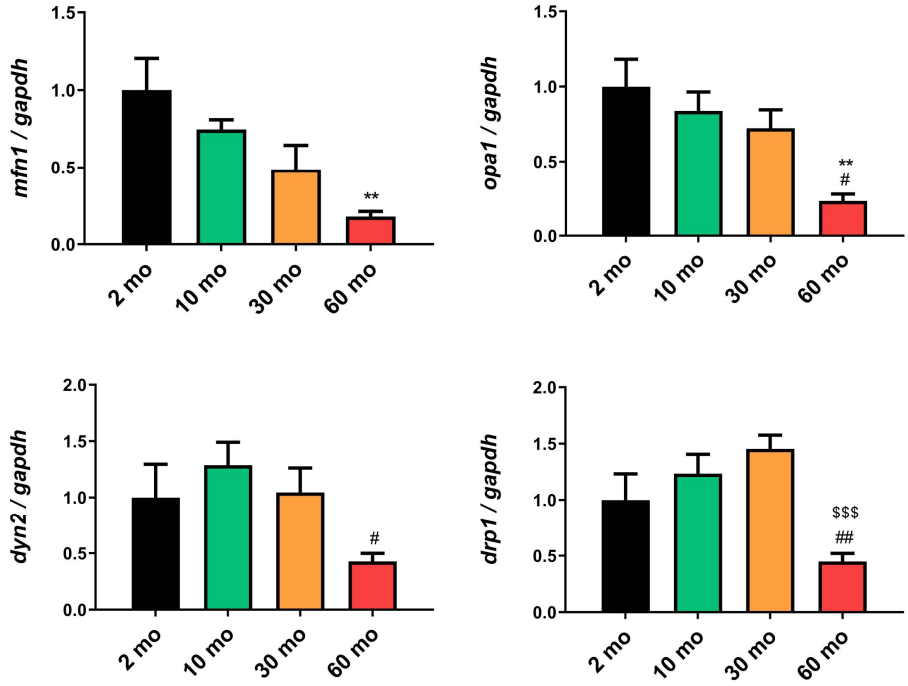

Figure 5. Reduction of mitochondrial dynamics in old fish. (**A**) y (**B**) The expression of mfn1 and opa1 exhibited a decreasing trend with age, becoming significant at 60 months (**C**) dyn2 expression increased at 10 months but also significantly decreased at 60 months (**D**) The expression of drp1 increased at 10 and 30 months but showed a substantial decrease at 60 months. Data are presented as mean ± SEM. ** $p < 0.01$ vs. 2 mo; # $p < 0.05$ vs. 10 mo; ## $p < 0.01$ vs. 10 mo; $$$ $p < 0.001$ vs. 30 mo. One-way ANOVA with a Tukey's post hoc test.

2.5. Confocal Analysis of Skeletal Muscle in Mito-GFP Zebrafish Shows Consistent Loss of Mitochondria with Age

Confocal analysis confirmed the TEM data, revealing the mitochondrial volume in the skeletal muscle of Mito-GFP zebrafish (Figure 6). In the younger groups (2 and 10 months), we observed a high GFP intensity in the muscle, indicating a higher number of mitochondria. By the time the fish reached 30 months of age, there was a significant reduction in the number of mitochondria within the muscle, and at 60 months, we observed a drastic reduction in the GFP signal.

 doi:10.20944/preprints202405.1073.v1

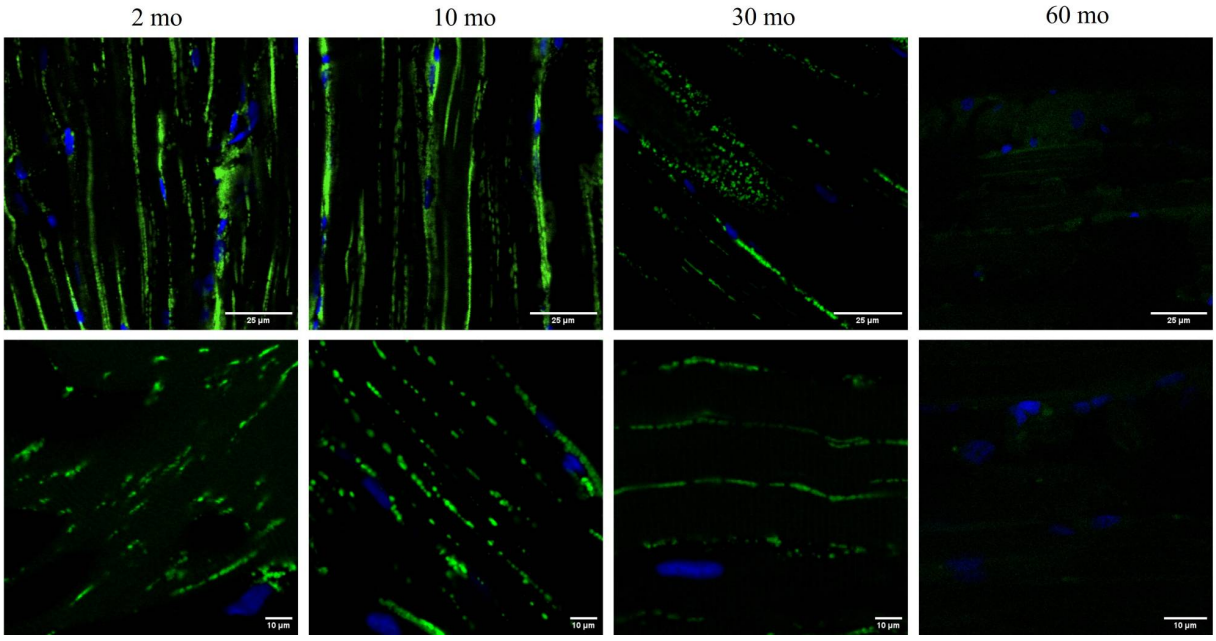

Figure 6. loss of mitochondria with age. Confocal microscopy images showed the nuclei labelled with DAPI and the mitochondria with GFP in the 2, 10, 30 and 60-month groups. The fish of 2 and 10 months exhibited a high GFP intensity, which started to diminish by 30 months and the signal disappeared at 60 months.

3. Discussion

With this study, we have demonstrated for the first time that zebrafish is a good model for studying the deterioration of skeletal muscle with age. The weakening of the skeletal muscle reached its maximum at the age of 60 months, which represents the highest lifespan of zebrafish under laboratory conditions [23,24]. Moreover, we proposed here to adapt, for the first time, the frailty index, which is commonly used to measure the degree of vulnerability in patients, primates, and mice [6,16]. Using morphometric and motor features, we calculated the frailty index, which increased with age. Hence, this index represents an initial, non-invasive step in the diagnosis of sarcopenia, which would subsequently require more specific and in-depth analyses. Our data support those of Rutkove et al., who used electrical impedance testing to detect muscle [25].

Concerning the skeletal muscle structure, previous studies reported a decrease in the cross-sectional area of muscle fibers and an increase in fibrosis in 21-month-old fish [15], whereas others detected D-galactose-induced sarcopenia in fish [14]. Here we also demonstrated age-dependent skeletal muscle atrophy. The number of myocytes and sarcomere length decreased with age, muscle ultrastructure was affected, and we observed muscle hypertrophy at 30 months, which preceded the loss of mass, along with a significant increase in collagen content at 60 months of age.

Muscle atrophy involves an imbalance in the protein degradation– synthesis process, with an excess of degradation [26]. In a study with 21-month-old fish, the authors observed a decrease in the IGF1/PI3K/Akt/mTOR protein synthesis signaling pathway and, conversely, an increase in the expression of genes and proteins associated with protein degradation, such as Murf, Fbxo32, FoxO, and the TRIM family, among others [15]. We have also demonstrated a decrease in the activation of this pathway with age, specifically a significant decline in Akt and p70S6K, that acts downstream of Akt [27], which correlates with the muscle atrophy found in histological analysis, likely due to an imbalance between protein synthesis and degradation. Furthermore, the TNF-α factor and activation of the NFκB pathway during aging also activate protein degradation. Furthermore, the TNF-α factor and activation of the NFκB pathway also activate protein degradation [28], revealing the role of inflammation in muscle atrophy, as demonstrated elsewhere [29–31].

Muscle atrophy was not only caused by the disruption of the IGF1/PI3K/Akt/mTOR pathway signaling but also by the observed decrease in myogenin expression in aged fish, which also contributes to muscle degeneration. Myogenin belongs to the family of myogenic regulatory factors (MRF), which are essential for muscle proliferation and differentiation. Specifically, myogenin is

 doi:10.20944/preprints202405.1073.v1

responsible for the fusion of myoblasts and their differentiation in both embryonic muscle development and adult muscle regeneration [32]. Recently, it has been shown in zebrafish that myogenin controls the number of resident muscle stem cells (MuSC), their location in the muscle, the rate of active and inactive MuSC, and the proper size of myofibers to maintain adult skeletal muscle homeostasis [20].

Parallel to the degeneration and loss of muscle mass during sarcopenia, there is a loss of function due to the replacement of fast muscle fibers responsible for muscle strength with slow fibers involved in endurance [33]. Prdm1a is a transcription factor that represses sox6, promoting the differentiation of slow muscle fibers, and it also directly represses the transcription of specific fast fiber genes [34]. We have observed an increase in the expression of prdm1a in 30 and 60-month-old fish, indicating a higher repression of sox6. As already observed, the absence of sox6 in zebrafish promotes the differentiation of slow fibers[22].

The bioenergetics of skeletal muscle depend on mitochondria, and mitochondrial dysfunction occurs during aging, which affects the oxidative capacity of the muscle [35]. In a model of D-galactose-induced sarcopenia in zebrafish, as well as in fish aged up to 21 months, they observed an increase in ROS in the muscle as well as a decrease in the expression of antioxidant factors such as SOD, GPx, and Nrf2 [14,15]. Since the mitochondria are the main source of ROS [36], this seemed to indicate mitochondrial dysfunction, which is indeed what they found: vacuolization, swelling, loss of mitochondrial cristae, rupture, a decrease in the number of mitochondria, and reduced mitochondrial respiration [14,15]. Our 60-month-old fish also showed a reduction in the number of IFM and their CSA, loss of cristae, vacuolization, and a 100% increase in mitochondrial damage. Furthermore, mitochondrial dynamics and biogenesis are essential for maintaining mitochondrial homeostasis [35]. In the two zebrafish sarcopenia models mentioned earlier, there was an alteration in mitochondrial fusion and fission events and a reduction in the AMPK/SIRT1/PGC-1α biogenesis pathway [14,15]. We also demonstrated a significant reduction in the expression of mitochondrial fusion and fission genes in older fish. Finally, mitochondria work together with SR to maintain Ca^{2+} homeostasis in skeletal muscle, which is crucial for both function and intracellular signaling. Moreover, an increase in Ca^{2+} within mitochondria leads to an increase in ROS [35]. Our results revealed mitochondrial damage and SR swelling with aging, which likely indicates an alteration in muscle Ca^{2+} metabolism.

Therefore, we demonstrated for the first time the physiopathology of sarcopenia in heavily aged fish, which resembles the characteristics of the disease seen in mammals. However, studies on sarcopenia in zebrafish are scarce. The primary limitation of our model and other models is the extended duration of the study. Nonetheless, we propose that zebrafish offer a valuable model for studying the mechanisms of skeletal muscle aging because of their significant advantages. They can absorb substances from water through their skin and gills, thus facilitating the use of induced sarcopenia models such as the dexamethasone model and the chronic alcohol model [37]. This also enables the testing of numerous drugs for sarcopenia treatment, which reflect an environmental model of disease. Nevertheless, the primary advantage that makes zebrafish highly useful for research is their ease of mutagenesis. Thanks to the CRISPR/Cas9 system, multiple genetic models of sarcopenia can be generated, allowing the study of several genes as therapeutic targets [37].

 doi:10.20944/preprints202405.1073.v1

4. Materials and Methods

4.1. Fish Maintenance and Experimental Groups

Mito-GFP adult zebrafish (Danio rerio) were provided by Kim et al. [38], and AB-strain adult zebrafish were provided by ZFBiolabs S.L (Madrid, Spain). The fish were maintained at the University of Granada's facility at a constant water temperature of 28.5 ± 1 °C, under a photoperiod of 14 h of light and 10 h of darkness (with lights turning on at 08:00 a.m.), using a recirculation aquaculture system provided by Aquaneering Incorporated (Barcelona, Spain). Fish feeding, breeding, maintenance, and anesthesia procedures adhered to established published protocols [39]. For age-dependent studies, we used zebrafish of 2, 10, 30, and 60 months of age. AB-strain zebrafish were used for the analysis of motor activity, frailty index, transmission electron microscopy, and optical microscopy. In addition, Mito-GFP zebrafish, characterized by EGFP-labeled cytochrome c oxidase (COXVIII), were used for confocal microscopy analysis.

All experiments were performed according to the National Institutes of Health Guide for the Care and Use of Laboratory Animals, the European Convention for the Protection of Vertebrate Animals used for Experimental and Other Scientific Purposes (CETS # 123), and the Spanish law for animal experimentation (R.D. 53/2013). The protocol was authorized by the Andalusian Ethical Committee (#29/05/2020/068).

4.2. Assessment of Locomotor Activity

The zebrafish were individually placed in a tank with aquarium system water and acclimated for four consecutive days before the experiment was conducted on the fifth day. Locomotor activity was recorded over a 20-min period, with a preceding 3-min adaptation stage, using a digital video tracking system consisting of a CCD camera connected to a computer. The acquired images were processed using SMART 3.0 software (Panlab Harvard Apparatus, Barcelona, Spain). The distance traveled (cm), mean speed (cm/s), and maximum speed (cm/s) of each fish were quantified.

4.3. Frailty Index Calculation

A clinical frailty index (FI) that has been validated in mice and primates was calculated using morphometric measures and physical activity as in humans [6,16]. Biometric parameters of zebrafish were evaluated by body weight and body length, and body mass index (BMI) was calculated as weight/length^2 (g/cm^2). The distance traveled (cm), mean speed (cm/s), and maximum speed (cm/s) of each fish were also used.

4.4. Gene Expression Analyses

Total RNA was extracted from skeletal muscle with TRI Reagent™ Solution (Thermo Scientific, Madrid, Spain) and electrophoresed in 1.5% agarose to check for RNA integrity. Total RNA was quantified in a NanoDrop by 260/280 nm absorbance, and reverse transcription was performed using a qScript cDNA Synthesis Kit (Quantabio, Beverly, Massachusetts, United States). Amplification was performed using quantitative real-time PCR in a Stratagene Mx3005P QPCR System (Agilent Technologies, Barcelona, Spain) according to the standard curve method with the PerfeCTa SYBR Green FastMix Low ROX (Quantabio, Beverly, Massachusetts, United States). gapdh housekeeping was used as an endogenous reference gene. Table 1 shows the primers used in the analysis.

Table 1. Forward and reverse sequencies of the primers used for PCR.

Gene	Primer Forward	Primer Reverse
mfn1	AACGAAGTGTGCTCTGCTCA	GGATTCAGAGTTCGCCACCA
opa1	AGACTGGAAGCAGAGGTGGA	GGAAGTGACGTCGAAAGAGC
drp1	AACATCCAGGACAGCGTACC	TCACCACAAGTGCGTCTCTC
dyn2	CGCAGATAGCAGTTGTCGGA	TCTGCTTCAATCTCCTGCCG
akt	TGCTGAAGAGTGACGGTACG	CTTTCTTCAGGCGTCTCCAC
p70s6k	CAGACTCCCGTTGACAGTCC	ATTGGACTGAGAGGCGTTCG
myogenin	CTCCACATACTGGGGTGTCG	GTCGTTCAGCAGATCCTCGT

 doi:10.20944/preprints202405.1073.v1

Gene	Primer Forward	Primer Reverse
prdm1a	TTGAACGCTTTGACATCAGC	GCTGCGATGAACTTTGATGA
gapdh	TCACACCAAGTGTCAGGACG	CGCCTTCTGCCTTAACCTCA

4.5. Skeletal Muscle Histology and Morphometric Analysis

Zebrafish samples were fixed for 48 h by embedding in 10% buffered formalin. After proper fixation, the fish samples were dehydrated by passing in ascending graded ethanol concentrations. The fish were then cleared in xylene and embedded longitudinally in paraffin. The paraffin blocks were trimmed until they reached the median plane of the fish where longitudinal 4-µm-thick sections of skeletal muscles were cut and mounted on glass slides. Following deparaffinization with xylene, the tissue sections were stained with hematoxylin and eosin (H&E) and Van Gieson stains (VG) to characterize skeletal muscle architecture and differentiate connective tissue and muscle fibers. All staining procedures were performed as described by Bancroft and Gamble. The sections were then mounted, covered, and examined, and digital images were obtained using a Carl Zeiss Primo Star Optic Microscope and a Magnifier AxioCam ICc3 digital camera (BioScience, Jena, Germany).

Morphometrical analyses of zebrafish skeletal muscle, including the number and width of myocytes, in addition to the percentage of collagen content, were performed on histological images using ImageJ software.

4.6. Transmission Electron Microscopy Analysis

Small pieces of skeletal muscle were dissected from the lateral part of the trunk region and rapidly fixed in 2.5% glutaraldehyde in 0.1 M cacodylate buffer (pH 7.4), followed by post fixation in 0.1 M cacodylate buffer with 1% osmium tetraoxide and 1% potassium ferrocyanide for 1 h. The specimens were immersed in 0.15% tannic acid for 50 s, incubated in 1% uranyl acetate for 1.5 h, dehydrated in ethanol, and then embedded in resin. Ultrathin sections were cut using a Reichert-Jung Ultracut E ultramicrotome, stained with uranyl acetate and lead citrate, and finally examined using a Carl Zeiss Leo 906E electron microscope.

Morphometrical analyses including length of sarcomeres, number, and cross-sectional area (CSA) of intermyofibrillar mitochondria (IFM), as well as number and CSA of subsarcolemmal mitochondria (SSM) were performed using TEM images and ImageJ processing software. These parameters were measured on area measured 5.15 µm width and 5.15 µm height.

4.7. Confocal Microscopy Analysis

Skeletal muscle was extracted from Mito-GFP zebrafish and fixed with 4% paraformaldehyde (PFA) for 5 h at 4 °C, and then washed in phosphate-buffered saline (PBS) for 10 min. Then, the skeletal muscle was incubated in 30% sucrose, which acts as an antifreeze, and washed again in PBS. The samples were mounted in optimal cutting temperature (OCT) medium, previously frozen in cold isopentane, which was cooled with liquid nitrogen and kept at −20°.

The skeletal muscle was cut longitudinally in 10µ sections in the cryostat, and the sections were recovered on superfrost microscope slides, which were kept at 4 °C. Then, the samples were then rehydrated in PBS for 10 min at RT and prepared with UltraCruz Aqueous Mounting Medium with DAPI (sc-24941, Santa Cruz Biotechnology, Dallas, Texas, United States). The images shown correspond to 1-micron-thick confocal sections obtained using a confocal laser scanning microscope at 120 and 200 magnifications (Nikon A1 confocal microscope, Centro de Instrumentación Científica, University of Granada).

4.8. Statistical Analysis

Statistical analyses were performed using GraphPad Prism 6 software (GraphPad, Software, Inc., La Jolla, CA, USA). Data are expressed as the mean ± S.E.M and one-way ANOVA with Tukey's post hoc test was used to compare the differences between the experimental groups. A *P* value of 0.05 was considered statistically significant.

Supplementary Materials: The following supporting information can be downloaded at the website of this paper posted on Preprints.org.

 doi:10.20944/preprints202405.1073.v1

Author Contributions: P.A.-M. and R.K.A.S., performed the experiments and analyzed the data; J.F.-M. and Y.R.-C. generated the figures and performed statistics; Y.Y., and G.E. wrote and edited the manuscript, D.A.-C. conceived the study, designed the experiments, and orchestrated the project. All authors have read and agreed to the published version of the manuscript.

Funding: The work was supported by grants no. CB16-10-00238 (ISCIII, Co-funded by European Regional Development Fund/European Social Fund "Investing in your future"), and no. P18-RT-698 (Junta de Andalucía, Consejería de Conocimiento, Investigación y Universidad).

Institutional Review Board Statement: The study was conducted in accordance with the National Institutes of Health Guide for the Care and Use of Laboratory Animals, the European Convention for the Protection of Vertebrate Animals used for Experimental and Other Scientific Purposes (CETS # 123), and the Spanish law for animal experimentation (R.D. 53/2013). The protocol was authorized by the Andalusian's Ethical Committee (#29/05/2020/068).

Informed Consent Statement: Not applicable.

Data Availability Statement: The datasets generated during and/or analyzed during the current study are available from the corresponding author (dacuna@ugr.es) on reasonable request. Materials described in the manuscript will be freely available to any research to use them for noncommercial purposes.

Conflicts of Interest: The authors declare no competing interests.

References

1. Cruz-Jentoft, A.J.; Sayer, A.A. Sarcopenia. The Lancet **2019**, 393, 2636–2646.
2. Angulo, J.; El Assar, M.; Rodríguez-Mañas, L. Frailty and Sarcopenia as the Basis for the Phenotypic Manifestation of Chronic Diseases in Older Adults. Mol Aspects Med **2016**, 50, 1–32.
3. Rogeri, P.S.; Zanella, R.; Martins, G.L.; Garcia, M.D.A.; Leite, G.; Lugaresi, R.; Gasparini, S.O.; Sperandio, G.A.; Ferreira, L.H.B.; Souza-junior, T.P.; et al. Strategies to Prevent Sarcopenia in the Aging Process: Role of Protein Intake and Exercise. Nutrients **2022**, 14.
4. Christian, C.J.; Benian, G.M. Animal Models of Sarcopenia. Aging Cell **2020**, 19.
5. Sayed, R.K.A.; de Leonardis, E.C.; Guerrero-Martínez, J.A.; Rahim, I.; Mokhtar, D.M.; Saleh, A.M.; Abdalla, K.E.H.; Pozo, M.J.; Escames, G.; López, L.C.; et al. Identification of Morphological Markers of Sarcopenia at Early Stage of Aging in Skeletal Muscle of Mice. Exp Gerontol **2016**, 83, 22–30, doi:10.1016/j.exger.2016.07.007.
6. Sayed, R.K.A.; Fernández-Ortiz, M.; Diaz-Casado, M.E.; Rusanova, I.; Rahim, I.; Escames, G.; López, L.C.; Mokhtar, D.M.; Acuña-Castroviejo, D. The Protective Effect of Melatonin Against Age-Associated, Sarcopenia-Dependent Tubular Aggregate Formation, Lactate Depletion, and Mitochondrial Changes. Journals of Gerontology - Series A Biological Sciences and Medical Sciences **2018**, 73, 1330–1338, doi:10.1093/gerona/gly059.
7. Sayed, R.K.A.; Fernández-Ortiz, M.; Diaz-Casado, M.E.; Aranda-Martínez, P.; Fernández-Martínez, J.; Guerra-Librero, A.; Escames, G.; López, L.C.; Alsaadawy, R.M.; Acuña-Castroviejo, D. Lack of NLRP3 Inflammasome Activation Reduces Age-Dependent Sarcopenia and Mitochondrial Dysfunction, Favoring the Prophylactic Effect of Melatonin. Journals of Gerontology - Series A Biological Sciences and Medical Sciences **2019**, 74, 1699–1708, doi:10.1093/gerona/glz079.
8. Fernández-Martínez, J.; Ramírez-Casas, Y.; Aranda-Martínez, P.; López-Rodríguez, A.; Sayed, R.K.A.; Escames, G.; Acuña-Castroviejo, D. IMS-Bmal1−/− Mice Show Evident Signs of Sarcopenia That Are Counteracted by Exercise and Melatonin Therapies. J Pineal Res **2023**, doi:10.1111/jpi.12912.
9. Andrews, J.L.; Zhang, X.; McCarthy, J.J.; McDearmon, E.L.; Hornberger, T.A.; Russell, B.; Campbell, K.S.; Arbogast, S.; Reid, M.B.; Walker, J.R.; et al. CLOCK and BMAL1 Regulate MyoD and Are Necessary for Maintenance of Skeletal Muscle Phenotype and Function. Proc Natl Acad Sci U S A **2010**, 107, 19090–19095, doi:10.1073/pnas.1014523107.
10. Zhu, P.; Hamlish, N.X.; Thakkar, A.V.; Steffeck, A.W.T.; Rendleman, E.J.; Khan, N.H.; Waldeck, N.J.; DeVilbiss, A.W.; Martin-Sandoval, M.S.; Mathews, T.P.; et al. BMAL1 Drives Muscle Repair through Control of Hypoxic NAD+ Regeneration in Satellite Cells. Genes Dev **2022**, 36, 149–166, doi:10.1101/gad.349066.121.
11. Aranda-martínez, P.; Fernández-martínez, J.; Ramírez-casas, Y.; Guerra-librero, A.; Rodríguez-santana, C.; Escames, G.; Acuña-castroviejo, D. The Zebrafish, an Outstanding Model for Biomedical Research in the Field of Melatonin and Human Diseases. Int J Mol Sci **2022**, 23.
12. Kishi, S.; Uchiyama, J.; Baughman, A.M.; Goto, T.; Lin, M.C.; Tsai, S.B. The Zebrafish as a Vertebrate Model of Functional Aging and Very Gradual Senescence. In Proceedings of the Experimental Gerontology; Elsevier Inc. **2003**; Vol. 38, pp. 777–786.

13. Daya, A.; Donaka, R.; Karasik, D. Zebrafish Models of Sarcopenia. DMM Disease Models and Mechanisms **2020**, 13.
14. Chen, Z.L.; Guo, C.; Zou, Y.Y.; Feng, C.; Yang, D.X.; Sun, C.C.; Wen, W.; Jian, Z.J.; Zhao, Z.; Xiao, Q.; et al. Aerobic Exercise Enhances Mitochondrial Homeostasis to Counteract D-Galactose-Induced Sarcopenia in Zebrafish. Exp Gerontol **2023**, 180, doi:10.1016/j.exger.2023.112265.
15. Sun, C.C.; Yang, D.; Chen, Z.L.; Xiao, J.L.; Xiao, Q.; Li, C.L.; Zhou, Z.Q.; Peng, X.Y.; Tang, C.F.; Zheng, L. Exercise Intervention Mitigates Zebrafish Age-Related Sarcopenia via Alleviating Mitochondrial Dysfunction. FEBS Journal **2023**, 290, 1519–1530, doi:10.1111/febs.16637.
16. Martinez De Toda, I.; Garrido, A.; Vida, C.; Gomez-Cabrera, M.C.; Viña, J.; De La Fuente, M. Frailty Quantified by the "Valencia Score" as a Potential Predictor of Lifespan in Mice. Journals of Gerontology - Series A Biological Sciences and Medical Sciences **2018**, 73, 1323–1329, doi:10.1093/gerona/gly064.
17. Cuthbertson, D.; Smith, K.; Babraj, J.; Leese, G.; Waddell, T.; Atherton, P.; Wackerhage, H.; Taylor, P.M.; Rennie, M.J. Anabolic Signaling Deficits Underlie Amino Acid Resistance of Wasting, Aging Muscle. The FASEB Journal **2005**, 19, 1–22, doi:10.1096/fj.04-2640fje.
18. Paturi, S.; Gutta, A.K.; Katta, A.; Kakarla, S.K.; Arvapalli, R.K.; Gadde, M.K.; Nalabotu, S.K.; Rice, K.M.; Wu, M.; Blough, E. Effects of Aging and Gender on Muscle Mass and Regulation of Akt-MTOR-P70s6k Related Signaling in the F344BN Rat Model. Mech Ageing Dev **2010**, 131, 202–209, doi:10.1016/j.mad.2010.01.008.
19. Bodine, SC; Stitt, TN; Gonzalez, M; Kline, WO; Stover, GL; Bauerlein, R; Zlotchenko, E; Scrimgeour, A; Lawrence, JC; Glass, DJ; Yancopoulos, GD. Akt/mTOR pathway is a crucial regulator of skeletal muscle hypertrophy and can prevent muscle atrophy in vivo. Nat Cell Biol **2001**, 3(11):1014-9. doi: 10.1038/ncb1101-1014
20. Ganassi, M.; Badodi, S.; Wanders, K.; Zammit, P.S. Myogenin Is an Essential Regulator of Adult Myofibre Growth and Muscle Stem Cell Homeostasis. Elife **2020**, 9, 1–23, doi:10.7554/eLife.60445.
21. Jackson, H.E.; Ingham, P.W. Control of Muscle Fibre-Type Diversity during Embryonic Development: The Zebrafish Paradigm. Mech Dev **2013**, 130, 447–457.
22. Jackson, H.E.; Ono, Y.; Wang, X.; Elworthy, S.; Cunliffe, V.T.; Ingham, P.W. The Role of Sox6 in Zebrafish Muscle Fiber Type Specification. Skelet Muscle **2015**, 5, doi:10.1186/s13395-014-0026-2.
23. Gerhard, G.S.; Kauffman, E.J.; Wang, X.; Stewart, R.; Moore, J.L.; Kasales, C.J.; Demidenko, E.; Cheng, K.C. Life Spans and Senescent Phenotypes in Two Strains of Zebrafish (Danio Rerio). Exp Gerontol **2002**, 37(8-9):1055-68. doi: 10.1016/s0531-5565(02)00088-8.
24. Kishi, S.; Slack, B.E.; Uchiyama, J.; Zhdanova, I. V. Zebrafish as a Genetic Model in Biological and Behavioral Gerontology: Where Development Meets Aging in Vertebrates - A Mini-Review. Gerontology **2009**, 55, 430–441.
25. Rutkove, SB; Chen, ZZ; Pandeya, S; Callegari, S; Mourey, T; Nagy, JA; Nath, AK. Surface Electrical Impedance Myography Detects Skeletal Muscle Atrophy in Aged Wildtype Zebrafish and Aged gpr27 Knockout Zebrafish. Biomedicines **2023**, 11(7):1938. doi: 10.3390/biomedicines11071938.
26. Park, S.S.; Kwon, E.-S.; Kwon, K.-S. Molecular Mechanisms and Therapeutic Interventions in Sarcopenia. Osteoporos Sarcopenia **2017**, 3, 117–122, doi:10.1016/j.afos.2017.08.098.
27. Zhong, Q.; Zheng, K.; Li, W.; An, K.; Liu, Y.; Xiao, X.; Hai, S.; Dong, B.; Li, S.; An, Z.; et al. Post-Translational Regulation of Muscle Growth, Muscle Aging and Sarcopenia. J Cachexia Sarcopenia Muscle **2023**, 14, 1212–1227.
28. Yoshida, T.; Delafontaine, P. Mechanisms of IGF-1-Mediated Regulation of Skeletal Muscle Hypertrophy and Atrophy. Cells **2020**, 9.
29. Bano, G.; Trevisan, C.; Carraro, S.; Solmi, M.; Luchini, C.; Stubbs, B.; Manzato, E.; Sergi, G.; Veronese, N. Inflammation and Sarcopenia: A Systematic Review and Meta-Analysis. Maturitas **2017**, 96, 10–15.
30. Pan, L.; Xie, W.; Fu, X.; Lu, W.; Jin, H.; Lai, J.; Zhang, A.; Yu, Y.; Li, Y.; Xiao, W. Inflammation and Sarcopenia: A Focus on Circulating Inflammatory Cytokines. Exp Gerontol **2021**, 154.
31. Liang, Z.; Zhang, T.; Liu, H.; Li, Z.; Peng, L.; Wang, C.; Wang, T. Inflammaging: The Ground for Sarcopenia? Exp Gerontol **2022**, 168.
32. Benavente-Diaz, M.; Comai, G.; Di Girolamo, D.; Langa, F.; Tajbakhsh, S. Dynamics of Myogenic Differentiation Using a Novel Myogenin Knock-in Reporter Mouse. Skelet Muscle **2021**, 11, doi:10.1186/s13395-021-00260-x.
33. Purves-Smith, F.M.; Sgarioto, N.; Hepple, R.T. Fiber Typing in Aging Muscle. Exerc Sport Sci Rev **2014**, 42(2):45-52. doi: 10.1249/JES.0000000000000012.
34. von Hofsten, J.; Elworthy, S.; Gilchrist, M.J.; Smith, J.C.; Wardle, F.C.; Ingham, P.W. Prdm1- and Sox6-Mediated Transcriptional Repression Specifies Muscle Fibre Type in the Zebrafish Embryo. EMBO Rep **2008**, 9, 683–689, doi:10.1038/embor.2008.73.
35. Bellanti, F.; Buglio, A. Lo; Vendemiale, G. Mitochondrial Impairment in Sarcopenia. Biology (Basel) **2021**, 10, 1–16.
36. Acuna-Castroviejo, D. Melatonin Role in the Mitochondrial Function. Frontiers in Bioscience **2007**, 12, 947, doi:10.2741/2116.

 doi:10.20944/preprints202405.1073.v1

37. Ichii, S.; Matsuoka, I.; Okazaki, F.; Shimada, Y. Zebrafish Models for Skeletal Muscle Senescence: Lessons from Cell Cultures and Rodent Models. Molecules **2022**, 27.
38. Kim, M.J.; Kang, K.H.; Kim, C.H.; Choi, S.Y. Real-Time Imaging of Mitochondria in Transgenic Zebrafish Expressing Mitochondrially Targeted GFP. Biotechniques **2008**, 45, 331–334, doi:10.2144/000112909.
39. Westerfield M. The Zebrafish Book. A Guide for the Laboratory Use of Zebrafish (Danio rerio). Univ Oregon Press, Eugene, OR, **2007**.